

A LOW PRESSURE REACTIVE ION ETCHING TECHNIQUE

A. Cetronio and G. Iannuzzi

SGS-Ates Componenti Elettronici S.p.A., Cascina Castelletto
20019 Settimo Milanese (MI), Italy.

Keywords: Reactive ion etching, anisotropy.

Compounds: Silicon, Poly-silicon, Silicon dioxide, freon + 4% oxygen.

ABSTRACT

Reactive ion etching of silicon and poly-silicon, under normal operating conditions (i.e. nominally 10-140 mTorr) with $CF_4 + 4\% O_2$ results in etch profiles with a certain amount of undercutting. By operating at lower pressures, in the range of 0.1 to 3 mTorr, near vertical wall etch profiles with silicon and poly-silicon have been obtained, with little to no reduction in the respective etch rates which are typically 260 and 370 Å/min at a pressure of 3×10^{-4} Torr.

1. INTRODUCTION

Of the many parameters which require further understanding before a reliable VLSI dry etch production process can be set up (1), perhaps the most important parameter is that of pattern delineation and its dependence on plasma pressure. Clearly, for best delineation an anisotropic etch process with a volatile reaction product is essential. A process which is very close to this ideal is reactive-ion etching with a fluorinate hydrocarbon gas such as CF_4 , CHF_3 , C_3F_8 , SF_6 etc. However even with this process, as a result of the operating pressures used (i.e. nominally 10 to 140 mTorr) the mean free path of the ions is of the same order of magnitude as the dark space sheath thus resulting in an isotropic etch process. Experimental confirmation of this model has been reported by K. Suzuki et al (2), using microwave frequencies to sustain a plasma discharge at a pressure of 5×10^{-4} Torr, obtaining good reproduction of the mask when etching a silicon substrate to a depth of approximately $1 \mu m$ with $CF_4 + 4\% O_2$ gas.

As reported below similar results have been obtained using r.f. instead of microwave excitation by means of a simple modification to a standard diode system (3), enabling plasma discharge initiation and sustainment at pressures as low as 1×10^{-4} Torr.

2. EXPERIMENTAL

A schematic representation of the system used is shown in fig. 1. A 27.2 MHz r.f. generator (maximum power output 2500 Watts) and the impedance matching network are connected between the water cooled aluminium cathode and the grounded chamber enclosure. The gas inlet and pumping port are 180° apart, situated below the diode system. To enable plasma initiation and sustainment at low pressures (i.e. < 1 mTorr), the system was modified such that a source of electrons other than those emitted through secondary emission by ions from the electrodes, is provided.

For low pressure operation in the range 0.1 to 10 mTorr the ionizing efficiency of the available electrons is increased by means of the magnetic field shown (3), which can be varied from 2.8×10^{-4} to 1×10^{-4} At/m. In fact for pressures in the range 0.1 to 1 mTorr maximum magnetic field is used, for pressures in the range 1 to 10 mTorr a field of 1×10^{-4} At/m is used and for pressures ≥ 10 mTorr the magnetic field is set to zero.

The substrates to be reactively ion etched are placed on the aluminium cathode whose area, used to convert input power to input power density, is 260 cm^2 . The gas pressure is measured with a capacitance manometer (M.K.S. Baratron) and the flow rate measured with a Brooks flow meter and controlled by means of a needle valve between the flow meter output and input to the vacuum chamber. The standard corrections appropriate to the gas are applied, and as illustrated in fig. 2 by varying the gas flow rate from 0.2 to 19 sccm (maintaining the pump speed constant) a pressure variation ranging from 3×10^{-4} to 1×10^{-1} Torr respectively is attained in the reaction chamber.

A line emission spectra (4) utilising an Oriel narrow-bandwidth interference type filter having a pass-band centred on a peak wave length of 7040 Å (corresponding to the fluorine spectral line) is used to monitor the end-point of etch processes. This device is also used as an indication of the concentration of active fluorine produced by the plasma discharge in the pressure range 3×10^{-4} to 1×10^{-1} Torr. A typical characteristic of the fluorine concentration (proportional to detector output current I_p) versus gas pressure in the reaction chamber for a load power of 100 Watts is illustrated in fig. 3. A qualitative explanation for this experimental result is as follows. In the range AB there is a gradual increase in active fluorine due to the corresponding increase in the number of CF_4 molecules. In this range due to confinement by the magnetic field and due to the large mean free path, electron energies are relatively high resulting in a finite value of dissociation cross section (5). In the range BC, the pressure is such that the electron mean free path is reduced and thus due to the increase in number of collisions the mean effective electron energy is reduced. At this reduced energy, $\sigma_d(\text{CF}_4)$ increases and with the increased concentration in CF_4 molecules and thus a maximum in the fluorine concentration is obtained. In the range CD the electron energy tends to the threshold

energy for dissociation (i.e. $\sim 15\text{eV}$) and thus the fluorine concentration decreases.

A d.c. bias versus system pressure characteristic is also illustrated on fig. 3. A qualitative explanation for this result is similar to that for the fluorine concentration, the only difference being that the ionization cross section must be considered instead of the dissociation cross section. The apparent anomaly of decreasing d.c. bias with increasing pressure in the range A'B' can be explained by the fact that in this region the dark sheath distance is inversely proportional to the square root of the concentration of gas molecules and thus the weighting factor for the d.c. bias.

Etch Rates

The etch rates of silicon, poly-silicon and SiO_2 (thermal) in $\text{CF}_4 + 4\% \text{O}_2$ were measured as a function of input power and varying system pressure. In the case of poly-silicon and SiO_2 the etch times for known thickness of material were measured by means of the endpoint detector. For silicon, the etch rate was measured by etching a wafer (masked with chrome) for a predetermined time and then measuring the etch thickness on a Talystep.

As illustrated in fig. 4 the etch rate of SiO_2 at a power density of 0.5 W/cm^2 and a pressure of 3×10^{-4} Torr is approximately 370 \AA/min , increasing to a maximum of 900 \AA/min at a pressure of 10 mTorr and then gradually decreasing with increasing pressure above 10 mTorr to a value of 670 \AA/min at 100 mTorr. This etch rate, considering that a low pressure is used, is well within practical values, being of the same order of magnitude as other reported results (3, 6, 7) utilizing pressures in the range 30-60 mTorr.

The etch rates of silicon and poly-silicon, illustrated in figures 5 and 6 respectively, follow a similar trend as with SiO_2 . For a power density of 0.5 W/cm^2 both attain a maximum in etch rate at a pressure of approximately 20 mTorr. Again the etch rate at low pressures (i.e. 3×10^{-4} Torr) is comparable with reported values for pressures in the range 30-60 mTorr (3, 6, 7).

Etch Profiles

The etch profiles on silicon, poly-silicon and SiO_2 were obtained by masking the respective substrates with chrome. The mask used was an Electromask Caliper 9 test reticle which enabled a study of fine geometries as small as $1 \mu\text{m}$. Figure 7 illustrates the various etch profiles obtained by operating in the low pressure region (i.e. 5×10^{-4} Torr) and also in the normal operating conditions (i.e. ~ 20 mTorr).

Etching of silicon at a pressure of ~ 20 mTorr results in slight undercutting (fig. 7a) when the substrate is placed on the cathode (i.e. RIE) and under similar conditions predominant undercutting (fig. 7b) when the substrate is placed on the anode of the diode system. For figure 7a the chrome mask is $\sim 2 \mu\text{m}$ wide with an etch depth of $\sim 2 \mu\text{m}$, and for fig. 7b the chrome mask is $\sim 2.5 \mu\text{m}$ wide with an etch

depth of $\sim 0.7 \mu\text{m}$.

The spike formation on the etched silicon substrate illustrated in fig. 7a has also been observed by Schwartz et al (8) and is attributed to residue formation of the non erodable mask which inadvertently covers portions of the substrate as a result of sputtering and redeposition of the etch mask.

Etching of silicon at a pressure of 5×10^{-4} Torr results in etch profiles with no undercutting as illustrated in fig. 7c and 7d. In fig. 7c the mask width is $\sim 2 \mu\text{m}$ with an etch depth of $\sim 1.5 \mu\text{m}$ and in fig. 7d the mask width is $\sim 1 \mu\text{m}$ with a similar etch depth. The abrupt change in the side wall taper as illustrated by both silicon etch profiles has also been observed by Schwartz et al. (8) and like these authors, we do not understand the cause and furthermore cannot predict when it will happen. Note that under low pressure conditions the spike formation on the etched silicon substrate is absent. An explanation for this phenomenon is that at lower pressures although sputtering of the mask is still present redeposition is much reduced thus eliminating completely the spike formation.

The results of poly-silicon are very similar to those for silicon and as illustrated in fig. 7e vertical walled etch profile is again obtained. In this case the mask width is $\sim 1.2 \mu\text{m}$ and the etch depth is $\sim 0.6 \mu\text{m}$.

As reported by other authors (8, 10) reactive ion etching of SiO_2 in the pressure range 20-100 mTorr results in a vertical wall etch profile. This is in agreement with our experimental observations and clearly no further change in etch profile is expected when operating at a pressure of 5×10^{-4} Torr. Figure 7f shows the etch profile of SiO_2 masked with chrome ($\sim 1 \mu\text{m}$ wide) and etched to a depth of $\sim 0.5 \mu\text{m}$.

3. DISCUSSION

From the experimental work it is apparent that the etch mechanism for silicon and poly-silicon in $\text{CF}_4 + 4\% \text{O}_2$ can be divided into three distinct regions depending on operating pressure. For low pressure operation (i.e. 3×10^{-4} to ~ 1 mTorr) the etch mechanism is primarily one of reactive ion sputtering. In the pressure range 1 mTorr to ~ 20 mTorr since the fluorine concentration has increased and since the d.c. bias is relatively high the etch mechanism is one of physical and chemical etching. In this region one would expect a certain amount of undercutting due to the isotropic nature of chemical etching, as illustrated in fig. 7a. For the pressure range 20 to 100 mTorr since the fluorine concentration is still relatively high and since the d.c. bias drops rapidly then chemical etching predominates tending to plasma etching conditions and thus isotropic etch profiles as shown in fig. 7b.

This latter mechanism also explains the reduction in etch rate for pressures > 20 mTorr, an experimental observation which is confirmed by Bondur's work (9).

In the case of SiO_2 , since the etch mechanism is one of ion assisted dissociation at the substrate surface (10), then it is expected that in the pressure range where the mean free path of the ions λ_i , is less than the dark space distance d_s , the etch profiles will have vertical walls. The condition for $\lambda_i \leq d_s$ holds true for pressures in the range of 100 mTorr and thus vertical walled etch profiles under reactive ion etching conditions are expected for the entire pressure range 5×10^{-4} to 100 mTorr. For pressure in excess of 100 mTorr SiO_2 etch profiles with undercutting have been obtained (11).

4. CONCLUSION

As illustrated by the experimental results, operating at low pressures in the range 5×10^{-4} to 1 mTorr, vertical walled etch profiles can be obtained for silicon, poly-silicon and SiO_2 etched in $\text{CF}_4 + 4\% \text{O}_2$. The advantage of operating under such conditions is that although the pressure is reduced by a factor of ~ 100 in comparison to normal reactive ion etch conditions the etch rates are still within acceptable production line values.

ACKNOWLEDGEMENTS

The authors would like to acknowledge Dr. M. Valente and Dr. F. Mori for their stimulating discussions during this work and Mr. G. Gambini for his assistance with the experimental work.

REFERENCES

- (1) R.G. Frieser, R.S. Harwarth and J.A. Bondur, Proc. 7th Intern. Vac. Congress and 3rd Int. Conf. Solid Surfaces 2, 1253 (1977).
- (2) K. Suzuki, et al, Jap. J. of Applied Phys., 16, 1979 (1977).
- (3) J.A. Bondur, J. Vac. Sci. Technol., 13, 1023 (1976).
- (4) R.G. Poulsen, J. Vac. Sci. Technol., 14, 266 (1977).
- (5) H.F. Winters, J.W. Coburn and E. Kay, J. Appl. Phys., 48, 4973 (1977).
- (6) H.W. Lehman and R. Widmer, Appl. Phys. Lett., 32, 1 (1978).
- (7) H.W. Lehman and R. Nidmer, J. Vac. Sci. Technol., 15, 319 (1978).
- (8) G.C. Schwartz, R.B. Rothman and T.J. Schopen, J. Electrochem. Soc., 126, 464 (1979).
- (9) J.A. Bondur, J. Electrochem. Soc., 126, 226 (1979).
- (10) J.W. Coburn and H.F. Winters, to be published.
- (11) A. Cetronio, to be published.

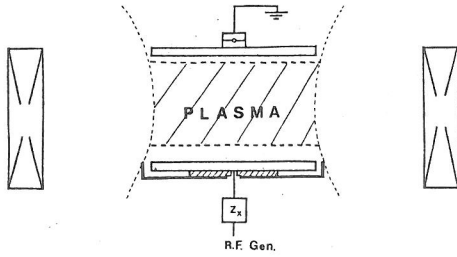


FIG. 1: A schematic presentation of the low pressure reactive ion etching system.

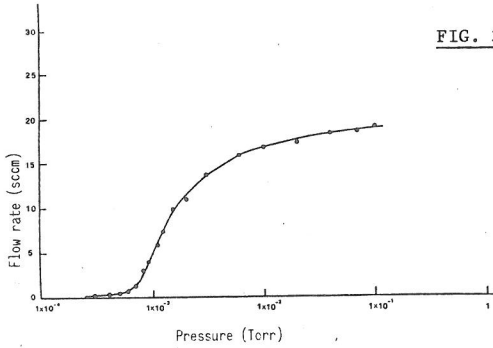


FIG. 2: Plot of $CF_4 + 4\% O_2$ flow rate versus pressure for a constant pumping speed.

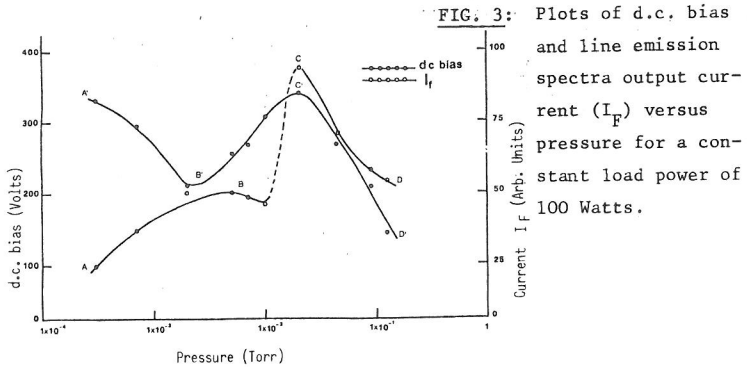


FIG. 3: Plots of d.c. bias and line emission spectra output current (I_F) versus pressure for a constant load power of 100 Watts.

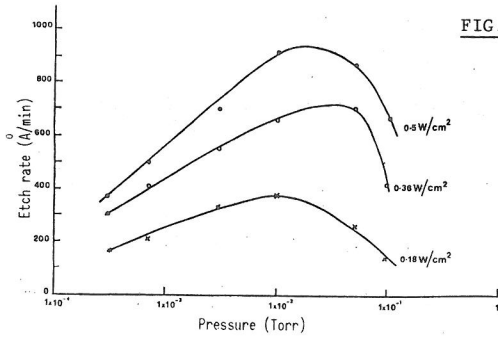


FIG. 4: SiO_2 etch rates versus pressure for varying power densities.

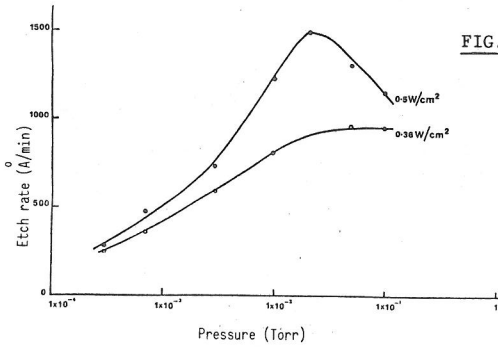


FIG. 5: Silicon etch rates versus pressure for varying power densities.

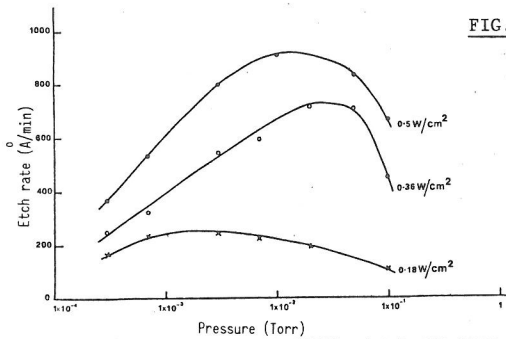


FIG. 6: Poly-silicon etch rates versus pressure for varying power densities.

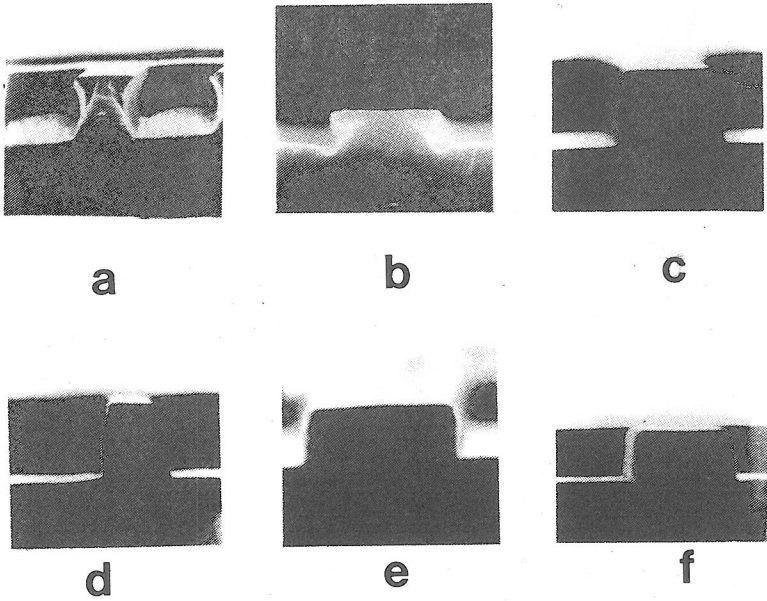


Fig. 7: Etch profiles for Silicon (a) to (d), poly-silicon (e), and SiO_2 (f) obtained at a power density of 0.36 W/cm^2 in $\text{CF}_4 + 4\% \text{ O}_2$.